International Journal of Heat and Fluid Flow 72 (2018) 304–316

Contents lists available at ScienceDirect

International Journal of Heat and Fluid Flow

journal homepage: www.elsevier.com/locate/ijhff

Outer shear layer characteristics of a radially expanding wall jet on smooth and dimpled surfaces

R. van Hout*[,a], V. Rinsky[a], C. Hershcovich[b], Y.J. Grobman[b]

[a] The Faculty of Mechanical Engineering, Technion-Israel Institute of Technology, Technion - city, Haifa, Israel
[b] The Faculty of Architecture and Town planning, Technion-Israel Institute of Technology, Technion - city, Haifa, Israel

ARTICLE INFO

Keywords:
Impinging jet
Dimpled surfaces
Primary-secondary vortex interaction
Self-similarity
Particle Image Velocimetry

ABSTRACT

Dimpled surfaces may enhance or decrease heat transfer compared to smooth surfaces. Here, the flow field of a round, axisymmetric air jet (diameter D) impinging on smooth and dimpled target surfaces (positioned at $H/D \approx 5$) was measured using particle image velocimetry (PIV). Reynolds numbers based on the jet exit velocity and D were, Re = 1,473, 6,322 and 12,438. Six different dimpled surfaces were investigated, subdivided in three pairs. In all cases, $D/d > 2$, where d is the dimple's opening size and $\delta/d \leq 1.0$, where δ is the dimple's depth. The focus was on the primary and secondary vortex interaction along the developing wall jet that was studied using the vorticity and the directional swirling strength. The latter were used to extract the vortex cores and subsequently their numbers, areas and circulation. The results showed that despite significant changes to the surface morphology as a result of the dimples, primary - secondary vortex interaction along the developing wall jet was similar as for the smooth plate. Furthermore, the normalized strength of secondary vortices peaked at $r/D \approx 2$, but differences between the plates became negligible away from the stagnation point at $r/D \approx 4$. In addition, it was shown that outer layer self-similarity was attained for the two highest Re. The present results indicate that within the present geometrical constraints, the outer shear layer characteristics of the wall jet generated by an impinging round jet on dimpled surfaces is not fundamentally different from those on a smooth surface.

1. Introduction

Turbulent impinging jets are commonly used in many different industrial applications such as for cooling electronic packages and turbine blades, drying textile and paper as well as cutting metal. An impinging jet issued from a converging, round nozzle changes from a high speed, nearly uniform flow having thin shear layers at the nozzle's exit to a transitional and fully developed radially expanding, turbulent wall jet after impingement. Typically three regions can be distinguished: (i) the free jet (Yule, 1978), (ii) the stagnation or impingement region (Geers et al., 2004) and (iii) the radially expanding wall jet (Knowles and Myszko, 1998; Krishnan and Mohseni, 2010; Banyassady and Piomelli, 2015). Each of these regions is characterized by different turbulence mechanisms making it difficult to perform accurate numerical simulations (Zuckerman and Lior, 2007). Adding to the complexity of the impinging jet's flow field and heat transfer characteristics is the dependency on a large number of parameters such as (i) the jet Reynolds number, $\mathrm{Re} = U_j D/\nu$, where U_j is the jet exit velocity, D the jet nozzle diameter, and ν is the fluid kinematic viscosity; (ii) the nozzle to plate distance, H/D, where H is the distance between the jet exit and the target plate (see Fig. 1); (iii) the jet exit velocity profile and turbulence level; (iv) the jet configuration (such as confined or not) and shape of the orifice. In addition, wall morphology, such as protrusions or indentations (dimples) may enhance or reduce the heat transfer.

The mechanism thought to be responsible for the high heat and mass transfer coefficients obtained by impinging jets is the interaction between primary and secondary vortices. The former are generated in the shear layer of the free jet as a result of Kelvin-Helmholtz instabilities and prior to break-up represent toroidal vortices encircling the jet's perimeter (Violato et al., 2012). The latter are generated by the action of the primary vortices upon impingement on the target surface. After impingement, the developing wall jet is characterized by partially overlapping inner and outer shear layers. It is thought that the latter is governed by the incoming turbulence of the free jet while the former develops close to the wall. The wall-normal position, z_m, of maximum radial velocity, U_m, represents an inner-layer scale while the wall jet's half width, $z_{1/2}$, defined as the position farthest away from the wall where the radial velocity equals $0.5U_m$, represents an outer layer scale.

While many studies have investigated jet impingement on smooth, flat target surfaces (Cooper et al., 1993; Nishino et al., 1996;

* Corresponding author.
E-mail address: rene@technion.ac.il (R. van Hout).

https://doi.org/10.1016/j.ijheatfluidflow.2018.06.011
Received 15 April 2018; Received in revised form 1 June 2018; Accepted 18 June 2018

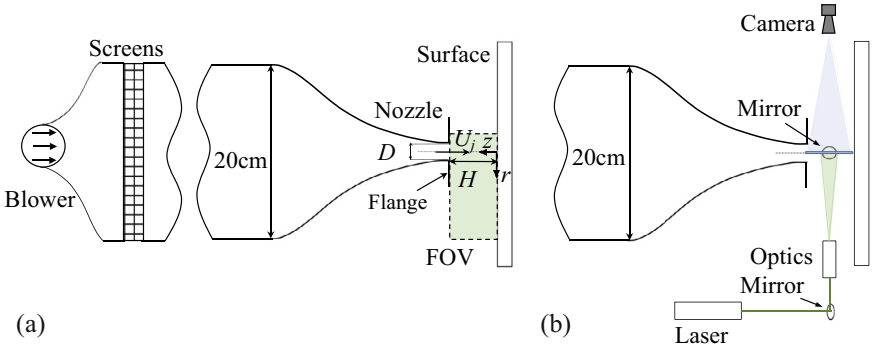

Fig. 1. Schematic layout of the experimental setup (Not to scale). (a) Side view, (b) Top view of PIV setup.

Fairweather and Hargrave, 2002; Hall and Ewing, 2006; Hadžiabdić and Hanjalić, 2008; Shademan et al., 2016), relatively little is known about the effect of varying surface roughness. The effect of target surface (sand-grain) roughness on the wall jet's inner and outer shear layer characteristics generated by a periodically forced jet ($H/D = 1$, Re = 66,000) was studied using large eddy simulations (LES) by Wu et al. (2016). They found that despite thickening of both inner and outer shear layers, vortex development along the target surface was similar to the smooth case with primary vortices decaying only slightly faster and secondary vortices having a slightly higher vorticity, compared to the smooth plate.

In this study, the focus is on bio-inspired, sculptured surfaces that in contrast to sand-grain roughness are characterized by "large-scale" dimples, known to enhance heat transfer in internal duct cooling applications (Chyu et al., 1997; Moon et al., 2003) and may be used to increase thermal performance of building envelopes (Grobman and Elimelech, 2016; Hershcovich et al., 2017). The published literature on jets impinging on dimpled surfaces can be classified as (i) single jet impingement onto a single dimple (Terekhov et al., 2006; 2009; Terekhov and Kalinina, 2011; Xie et al., 2013; Hashiehbaf et al., 2015; Zhang et al., 2015), (ii) single jet impingement on a dimpled surface (Ortega-Casanova and Granados-Ortiz, 2014) and (iii) jet arrays impinging on a dimpled surface (Azad et al., 2000; Ekkad and Kontrovitz, 2002; Kanokjaruvijit and Martinez-Botas, 2010). In case (i), heat transfer enhancement as well as suppression has been achieved when the ratio between the jet diameter and the dimple diameter, D/d, was < 1 (Terekhov et al., 2009; Xie et al., 2013) and > 1 (Xie et al., 2013), respectively. Literature results on heat transfer of jet arrays impinging on dimpled surfaces (case (iii)) lack consensus and both suppression (Ekkad and Kontrovitz, 2002) and enhancement (Azad et al., 2000; Kanokjaruvijit and Martinez-Botas, 2010) have been reported.

A single round jet impinging on a dimpled surface (case (ii)) and in particular the development of the radial wall jet has hardly been studied. Numerical simulation results ($7{,}000 < \mathrm{Re} < 19{,}000$, $H/D > 5$, $D/d = 2$) by Ortega-Casanova and Granados-Ortiz (2014) indicated that at the stagnation point, heat transfer can be enhanced or at least be as good as the flat plate case regardless of stand-off distance and if the jet included swirl or not. Furthermore, in most cases dimpled surfaces enhanced global heat transfer. Their results mainly displayed average Nusselt numbers and no detailed flow field information was reported. To the best of the authors' knowledge, there are no published measurements of the heat transfer nor flow field characteristics of a single round jet impinging on a dimpled surface.

The goal of the present study is to measure the flow field of a single round jet impinging on different dimpled target surfaces using particle image velocimetry (PIV). In particular, the effect of different dimple geometries on the wall jet's outer shear layer characteristics and on primary-secondary vortex interaction was studied. The experimental setup and data processing is described in Section 2 while the comparison between jet impingement on smooth and dimpled target surfaces is presented in Section 3. A summary and discussion is given in Section 4.

2. Experimental setup and data processing

The round jet was issued from a contraction attached to the exit of a windtunnel test section (van Hout et al., 2018) that smoothly changed from a square cross-section (20×20 cm^2) to a round circular jet ($D = 20$ mm, contraction area ratio of 100:1, Fig. 1). The air jet impinged on a vertically placed gypsum surface (20×20 cm^2) at a stand-off distance, $H/D \approx 5$. Besides a smooth target surface, three pairs of dimpled target surfaces were designed and 3D printed (Table 1). In the first pair (1-25, 1-50 R-Round) dimples have the same spherical shape but are differently scaled while pairs II (R-REC and R-TRI) and III (S-REC and S-TRI) have the same dimple opening size and shape but have different internal dimple geometry. In all cases, $D/d > 2$ while the ratio between the dimple depth and opening size, δ/d, equaled 0.816 or 1.0 (Table 1). Experiments were performed at three mean jet exit velocities, $U_j = 1.16 \pm 0.07$, 4.99 ± 0.01 and 9.83 ± 0.05 m/s corresponding to jet Reynolds numbers of $\mathrm{Re} = 1{,}473 \pm 96$, $6{,}322 \pm 44$ and $12{,}438 \pm 132$. Accurate experimental conditions for each target surface are summarized in Table 1. A schematic system layout including the right-handed cylindrical coordinate system is depicted in Fig. 1, where r, z denote the radial and longitudinal directions, respectively; θ (not shown) denotes the azimuthal direction. Corresponding instantaneous velocities are denoted by U_r, U_θ and U_z and fluctuating (Reynolds decomposed) velocities by u_r, u_θ and u_z; Angle brackets, $\langle .. \rangle$, denote ensemble averaged values and a prime " ′ " denotes the root-mean-square (rms) value. Bold typeface denotes vectors.

The flow field was measured using a PIV system comprising a CCD camera (2048×2048, 7.4×7.4 μm^2 pixels), an Nd:Yag laser (Litron lasers, Nano-L, 200 mJ/pulse at 15 Hz), laser sheet optics and data acquisition/processing software (DaVis 8.1, LaVision GmbH). The laser sheet (1 mm thick) vertically crossed the jet's centerline (Fig. 1b). The camera's field of view (FOV) was 100×130 mm^2, covering the jet, the impingement region and part of the radially expanding wall jet. The flow field inside the dimples was not measured due to lack of optical access. Tracer particles (0.2–0.3 μm diameters, glycerine BP/purified water mixture "Smoke Fluid A", Concept Engineering Limited) were generated by a portable smoke generator (Colt 4) and introduced at the blower's entrance to ensure a spatially uniform distribution at the nozzle exit. At each Re and for each target surface, five data sets were acquired at an acquisition rate of 7 Hz, totaling 450 statistically independent pairs of PIV images. These were processed using a multi-pass algorithm based on the fast Fourier transform (FFT, DaVis 8.1) starting with an interrogation window size of 64×64 pixels that was reduced in the final step to 16×16 pixels with 50% overlap resulting in a vector spacing of 0.51 mm. In between passes, outlier detection was performed and the vector maps were smoothed using a 3×3 Gaussian spatial filter (Adrian and Westerweel, 2011).

The accuracy of an instantaneous velocity measurement using PIV depends on several different contributions such as the tracer particle response time, image distortions, spatial resolution and out-of-plane motion (Adrian and Westerweel, 2011). Errors as a result of the finite